

6D Phase-Space Manipulation of High Brightness Electron Beams

Yine Sun

Advanced Photon Source

Argonne National Lab.

Beam Dynamics Workshop

Institute for Pure & Applied Mathematics

University of California Los Angeles

Jan. 26, 2017

Outline

- Introduction to Phase Space, Emittance and Transfer Matrix
- Round-to-Flat Beam Transformation
 - Theory;
 - Experimental demonstration.
- Transverse-to-longitudinal Emittance EXchange (EEX)
 - Theory;
 - Experimental demonstration;
 - Longitudinal phase-space shaping via EEX.
- A Further Step
 - Double EEX;
 - Round-to-Flat Combined with EEX.
- Summary

Phase Space and Emittance

□ The common coordinate system used in particle accelerator physics is the Cartesian system (x,y,z) :

- Longitudinal coordinate $z \rightarrow$ along particle propagation direction;
- Transverse coordinates x and $y \rightarrow$ Horizontal x and vertical y .

□ Particle position (x,y,z) combined with its momentum (p_x,p_y,p_z) form its coordinates in the 6D phase space (x,p_x,y,p_y,z,p_z) :

- Each particle is represented by a point, and all particles in a bunch occupy a volume.

□ A figure of merit of the beam's projection in (x,p_x) subspace is the **normalized rms emittance** defined as:

$$\varepsilon_x^n = \frac{1}{mc} \sqrt{\langle x^2 \rangle \langle p_x^2 \rangle - \langle xp_x \rangle^2}$$

□ **Liouville's theorem**: for non-interactive particles, the volume occupied by a certain number of particles in the 6D phase space is constant.

$$\varepsilon_x^n \varepsilon_y^n \varepsilon_z^n = \text{Const}$$

Trace Space and un-normalized emittance

□ More extensively used are the derivatives of (x,y) with respect to z :

- $x' = P_x/P_z, y' = P_y/P_z$

- 4D Coordinate vector $U = \begin{bmatrix} x \\ x' \\ y \\ y' \end{bmatrix}$

□ Un-normalized emittance

$$\varepsilon_x = \sqrt{\langle x^2 \rangle \langle x'^2 \rangle - \langle xx' \rangle^2}$$

□ For relativistic beams (relativistic factors β and γ) with low energy spread, we have

$$\varepsilon_x = \frac{\varepsilon_x^n}{\beta\gamma}$$



Transfer Matrix

- The transverse motion of a particle in an accelerator without dissipative force can be written as the *Hill's equation*:

$$u'' + K(z)u = 0 \text{ where } u \text{ can be } x \text{ or } y.$$

- Suppose $A(z)$ and $B(z)$ are two independent solutions which satisfy the following boundary conditions:

$$A(z_0) = B'(z_0) = 1$$

$$A'(z_0) = B(z_0) = 0$$

- Any solution to the equation can be written as

$$\begin{bmatrix} u(z) \\ u'(z) \end{bmatrix} = \begin{bmatrix} A(z) & B(z) \\ A'(z) & B'(z) \end{bmatrix} \begin{bmatrix} u(z_0) \\ u'(z_0) \end{bmatrix} \equiv M(z|z_0) \begin{bmatrix} u(z_0) \\ u'(z_0) \end{bmatrix}$$

Transfer matrix from z_0 to z

Transfer Matrix: Properties and Examples

- The 2D transfer matrix can be extended to 6D.
- The determinant of the transfer matrix is unity.
- For a Hamiltonian system, the transfer matrix satisfies the *symplectic* condition. In 6D:

$$\widetilde{M}_6 J_6 M_6 = J_6, \text{ where } J_6 = \begin{bmatrix} J & 0 & 0 \\ 0 & J & 0 \\ 0 & 0 & J \end{bmatrix} \text{ and } J = \begin{bmatrix} 0 & 1 \\ -1 & 0 \end{bmatrix} \text{ is the 2x2 unit symplectic matrix.}$$

- For a constant $K(z) = k$
 $u'' + ku = 0$

- If $k > 0$

$$M(z|z_0) = \begin{bmatrix} \cos \varphi & \frac{\sin \varphi}{\sqrt{k}} \\ -\sqrt{k} \sin \varphi & \cos \varphi \end{bmatrix} \text{ Focusing quad: } \varphi = (z_1 - z_0)\sqrt{k}$$

- If $k < 0$

$$M(z|z_0) = \begin{bmatrix} \cosh \varphi & \frac{\sinh \varphi}{\sqrt{|k|}} \\ \sqrt{|k|} \sinh \varphi & \cosh \varphi \end{bmatrix} \text{ Defocusing quad: } \varphi = (z_1 - z_0)\sqrt{|k|}$$

- If $k = 0$

$$M(z|z_0) = \begin{bmatrix} 1 & z_1 - z_0 \\ 0 & 1 \end{bmatrix} \text{ Drift space}$$



Beam Matrix

- Consider a bunch of particles centered at the origin of the phase space, i.e., $\langle x_i \rangle = 0$ etc. where $\langle \quad \rangle$ represents taking the average;
- Beam matrix: the covariance matrix of the phase space coordinates U ; for (x, x', y, y') subspace:

$$\Sigma = \langle U \tilde{U} \rangle = \begin{bmatrix} \langle x^2 \rangle & \langle x x' \rangle & \langle x y \rangle & \langle x y' \rangle \\ \langle x' x \rangle & \langle x'^2 \rangle & \langle x' y \rangle & \langle x' y' \rangle \\ \langle y x \rangle & \langle y x' \rangle & \langle y^2 \rangle & \langle y y' \rangle \\ \langle y' x \rangle & \langle y' x' \rangle & \langle y' y \rangle & \langle y'^2 \rangle \end{bmatrix}$$

Emittance is the determinant of the beam matrix.

- The beam matrix propagates via

$$\Sigma(z) = M \Sigma(z_0) \tilde{M}$$

where M is the transfer matrix from z_0 to z .

Phase-Space Manipulation



Phase-Space Manipulation

- ❑ An electron beam directly out of a photoinjector does not always have the phase-space properties required in its applications.
- ❑ Phase-space manipulation is necessary to achieve certain beam distribution, for example:
 - the beam can be **compressed longitudinally** → higher peak current → FELs;
 - round beam → **flat beam** (to drive planar dielectric wakefield or planar radiation generation gratings etc...);
 - the longitudinal and transverse **Emittances** of the beam can be **EXchanged (EEX)**;
 - when EEX is combined with the flat beam → **repartition of emittances in 3D** can be achieved;
 - the above manipulations are in the root-mean-square sense; the beam profiles can be more **precisely tailored**, such as bunch train or linearly ramped current etc. for higher transformer ratio in a wakefield accelerator etc.
- ❑ Aside from beam applications, other possible applications include beam diagnostics, bunch compression etc.

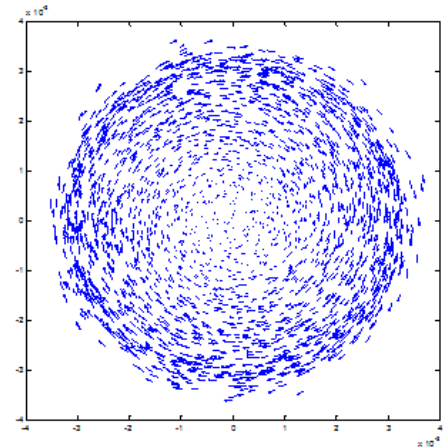
Round-to-Flat Beam Transformation



Round-to-flat beam transformation: Beam Matrix Formulation

$$\Sigma_{round} = \begin{bmatrix} \varepsilon_{eff} \beta & 0 & 0 & L \\ 0 & \varepsilon_{eff} / \beta & -L & 0 \\ 0 & -L & \varepsilon_{eff} \beta & 0 \\ L & 0 & 0 & \varepsilon_{eff} / \beta \end{bmatrix}$$

General form of the beam matrix of a round beam at waist location.

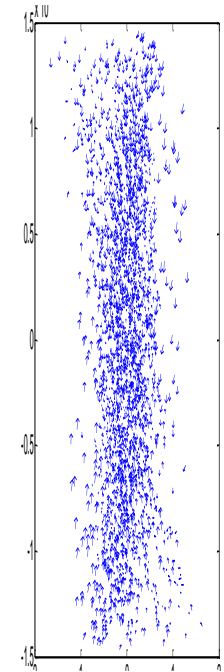


$$\Sigma_{flat} = M \Sigma_{round} \tilde{M}$$

Going through a round-to-flat beam transformation matrix M which is symplectic

$$\Sigma_{flat} = \begin{bmatrix} \varepsilon_- \beta & 0 & 0 & 0 \\ 0 & \varepsilon_- / \beta & 0 & 0 \\ 0 & 0 & \varepsilon_+ \beta & 0 \\ 0 & 0 & 0 & \varepsilon_+ / \beta \end{bmatrix}$$

Beam is decoupled in x and y and a flat beam with emittance ε_- and ε_+ is generated.



Invariants of the Symplectic Transformation

$$I_1 = \varepsilon_{4D} = \sqrt{|\Sigma|} \Rightarrow \varepsilon_+ \varepsilon_- = \varepsilon_{eff}^2 - L^2$$

$$I_2 = -\frac{1}{2} \text{Trace}(J_4 \Sigma J_4 \Sigma) \Rightarrow \varepsilon_+^2 + \varepsilon_-^2 = 2(\varepsilon_{eff}^2 + L^2)$$

K.-J. Kim, Phys. Rev. St. Accel Beams **6**, 104002 (2003).

Round beam emittance:

$$\varepsilon_{eff} = \sqrt{\varepsilon_u^2 + L^2}$$

uncorrelated emittance

Const. related to canonical angular momentum $L = \frac{\langle L \rangle}{2Pz}$

Flat beam emittances are given by:

$$\varepsilon_{\pm} = \sqrt{\varepsilon_u^2 + L^2} \pm L$$

e.g. $L=20 \mu\text{m}$, $\varepsilon_u=1 \mu\text{m}$
 $\varepsilon_+=47 \mu\text{m}$; $\varepsilon_-=0.02 \mu\text{m}$

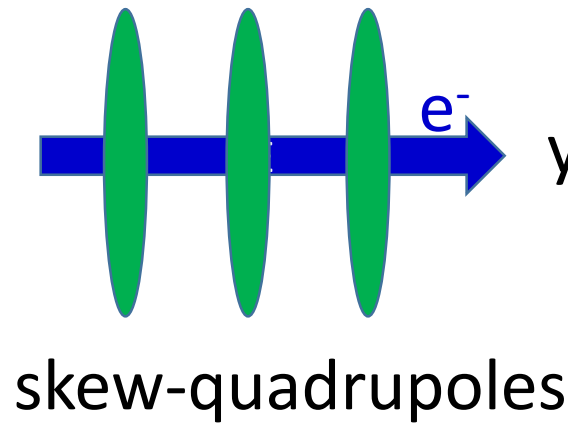
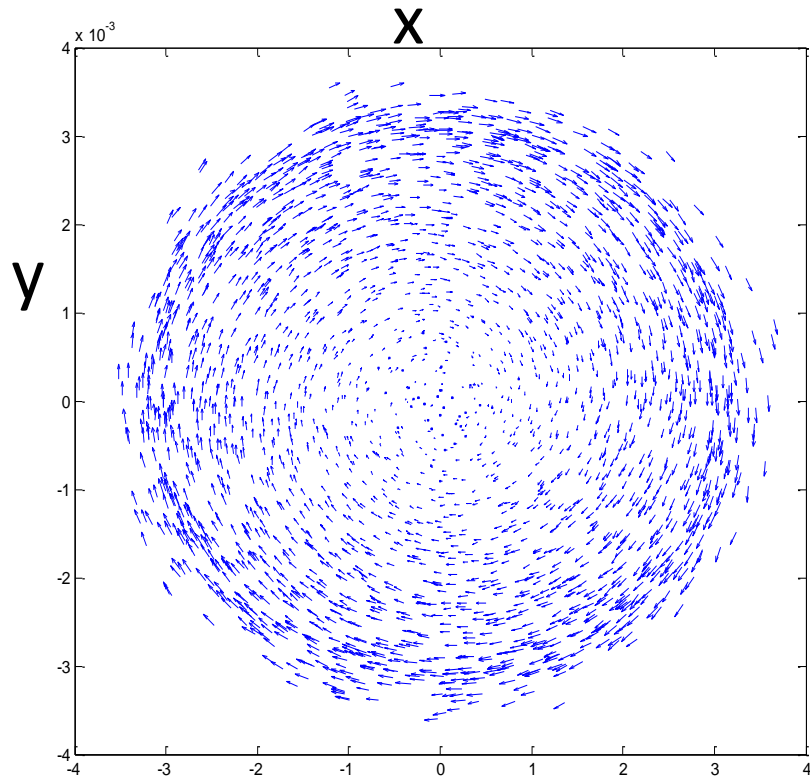
For $L \gg \varepsilon_u$, $\varepsilon_- = \frac{\varepsilon_u^2}{2L} \ll \varepsilon_u$

Flat beam emit. could be smaller than thermal emit.

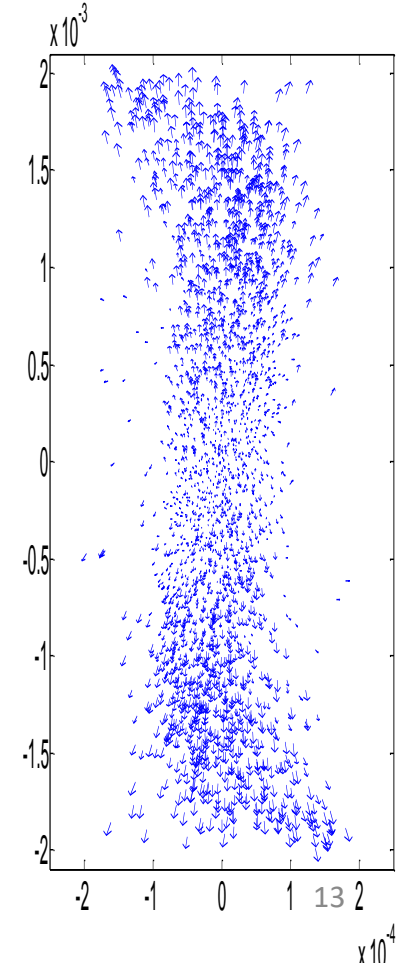
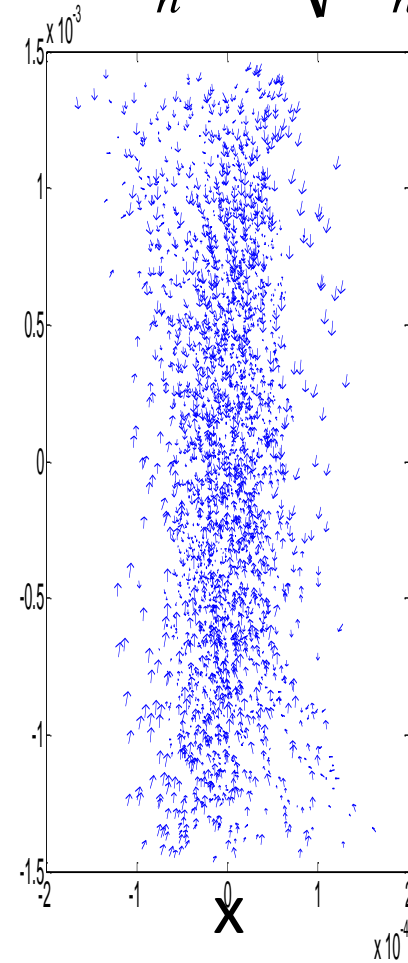
Round-to-Flat Beam Transformation

1 Generation of an angular-momentum-dominated beam by immersing the cathode in a high longitudinal magnetic field;

2 Removal of the angular momentum via a set of quadrupoles to obtain a flat beam.



$$\varepsilon_n^\pm = \sqrt{\varepsilon_n^2 + L^2} \pm L$$



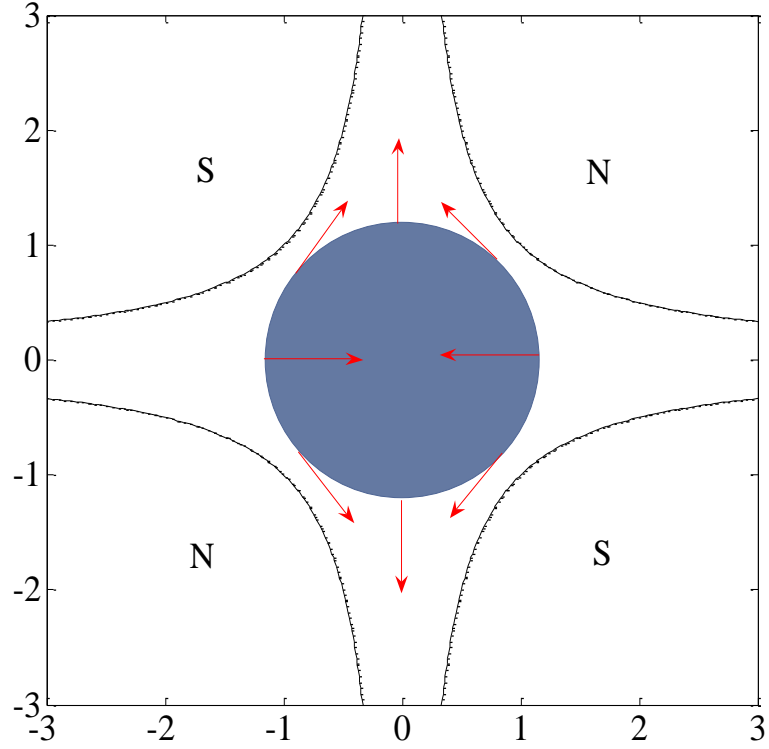
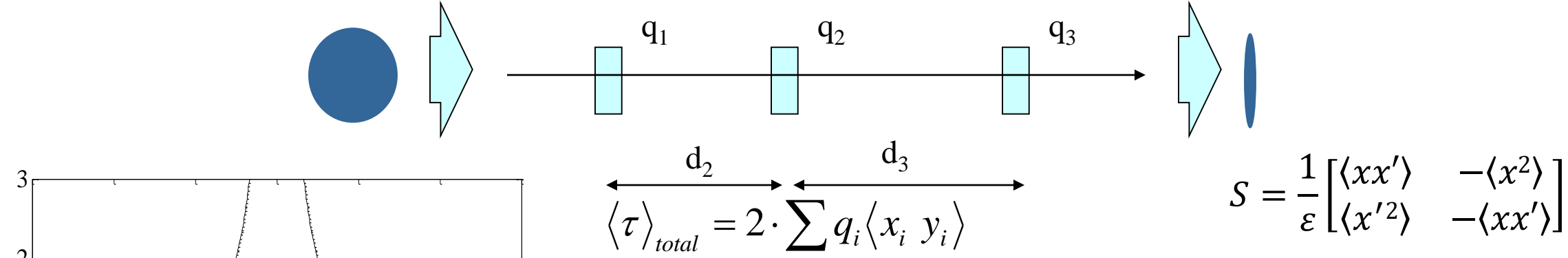
Ya. Derbenev, University of Michigan Report No. UM-HE-98-04 (1998).

R. Brinkmann et al., PRSTAB 4, 053501 (2001).

Round-to-flat transfer matrix building blocks: skew quads and drifts

Round beam: emittance ratio =1 but with large x-y coupling via angular momentum.

Flat beam: large transverse emittance ratio, zero average angular momentum.



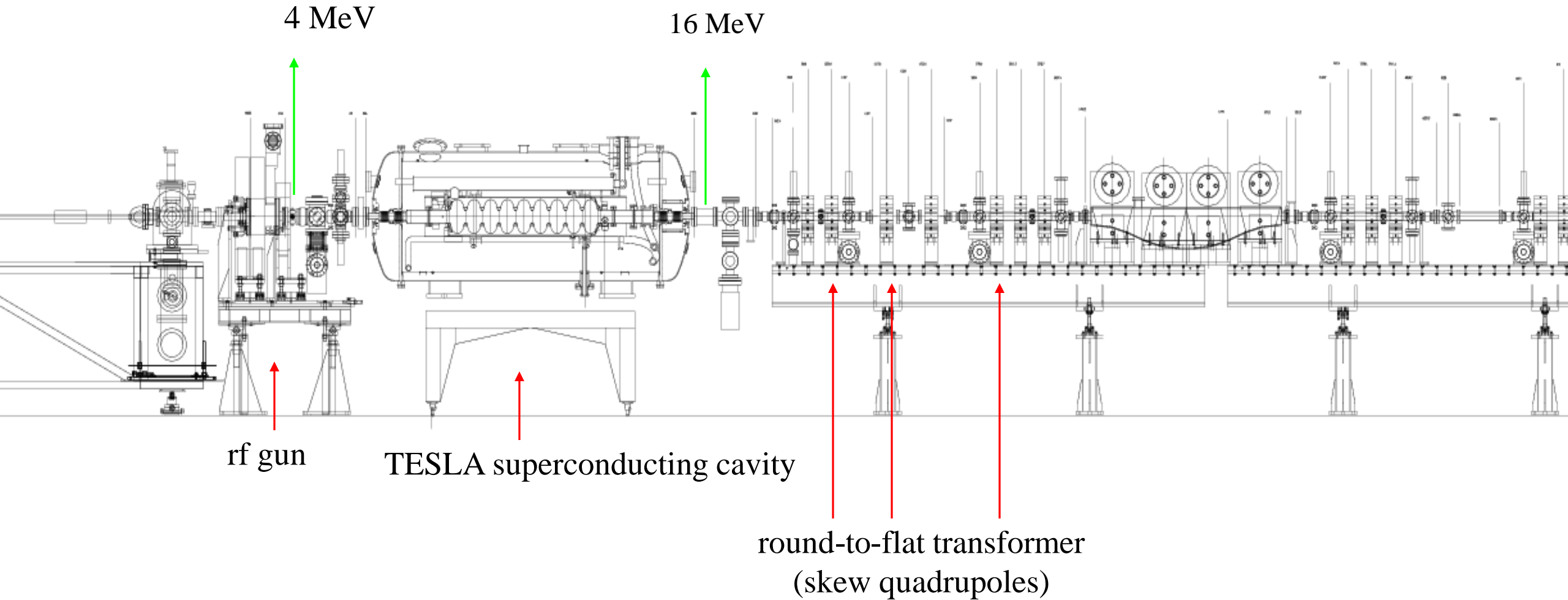
Two sets of solutions:

$$q_1 = \pm \sqrt{\frac{-d_2 S_{11} + S_{12} - d_2 d_T S_{21} + d_T S_{22}}{d_2 d_T S_{12}}}$$

$$q_2 = -\frac{S_{12} + d_T S_{22}}{d_2 d_3 (1 + S_{12} q_1)} \quad \text{(D. Edwards)}$$

$$q_3 = -\frac{q_1 + q_2 + d_2 S_{11} q_1 q_2 + S_{21}}{1 + (d_T q_1 + d_3 q_2) S_{11} + d_2 d_3 q_2 (S_{21} + q_1)}$$

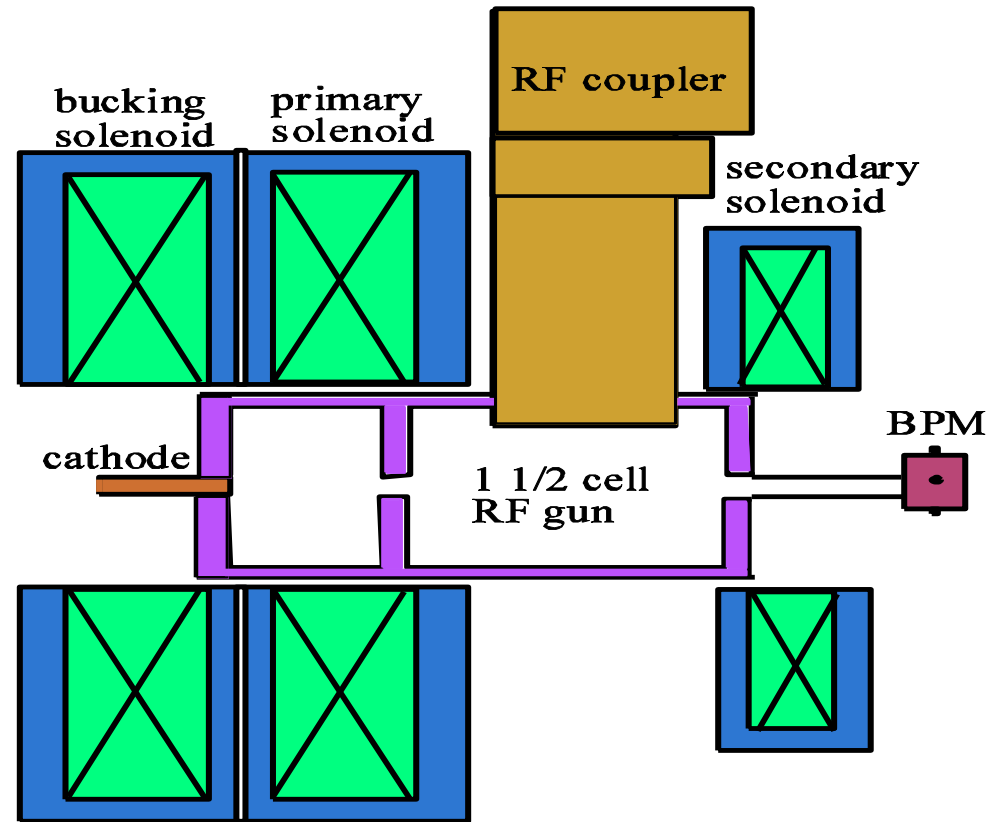
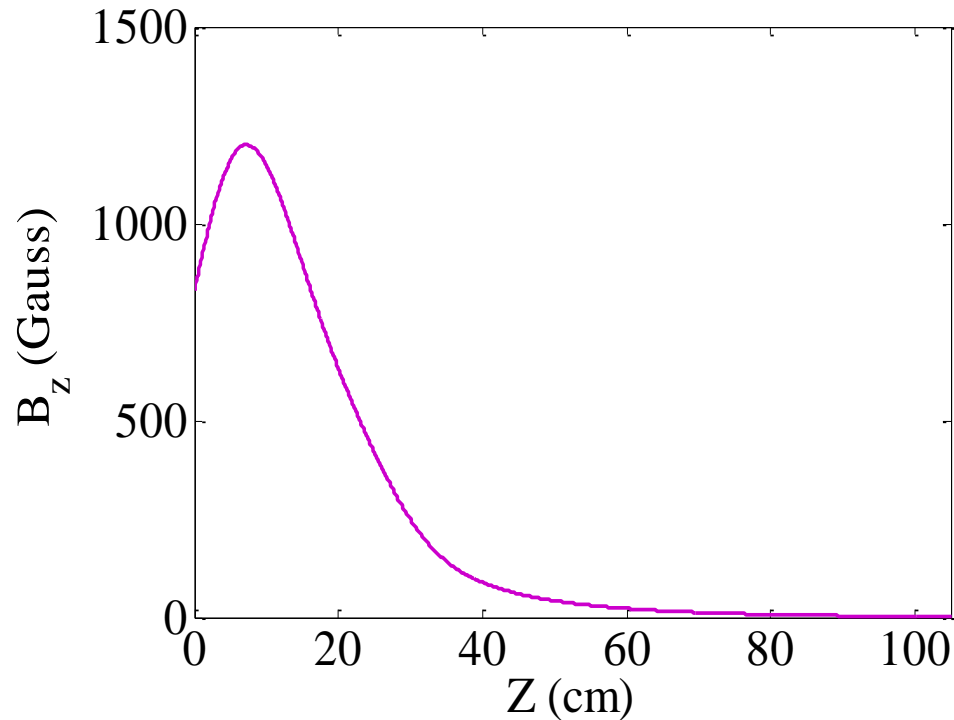
Round-to-Flat Beam Transformation Demonstration: Fermilab/NICADD Photoinjector Lab. (FNPL) (a.k.a. A0)



Generation of angular momentum dominated e⁻ beam

$$L = \gamma m r^2 \dot{\phi} + \frac{1}{2} e B_z r^2$$

On the photocathode: $\langle L \rangle = e B_0 \sigma_c^2$



FNPL 1.625-cell RF gun, 1.3 GHz

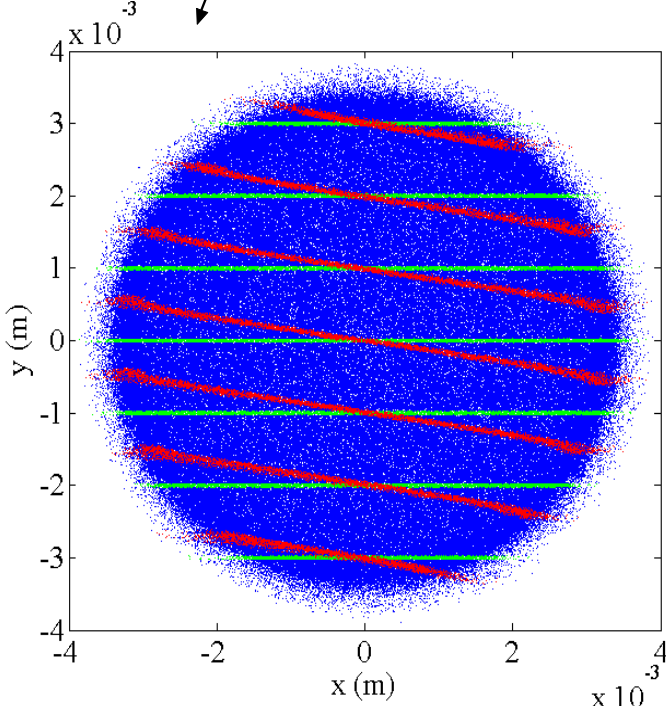
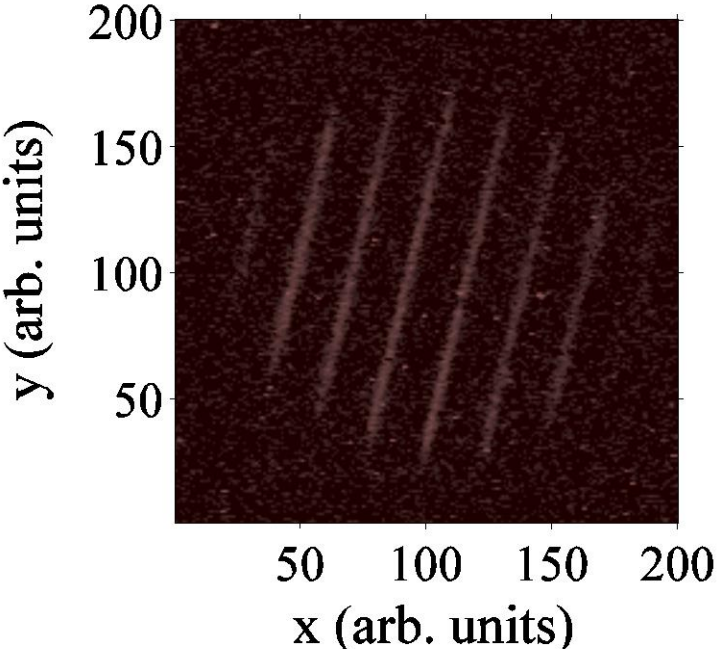
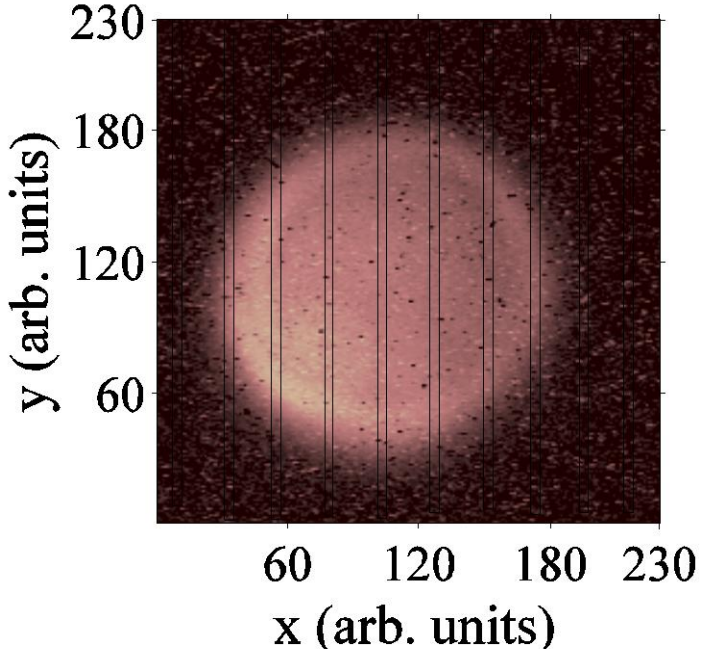
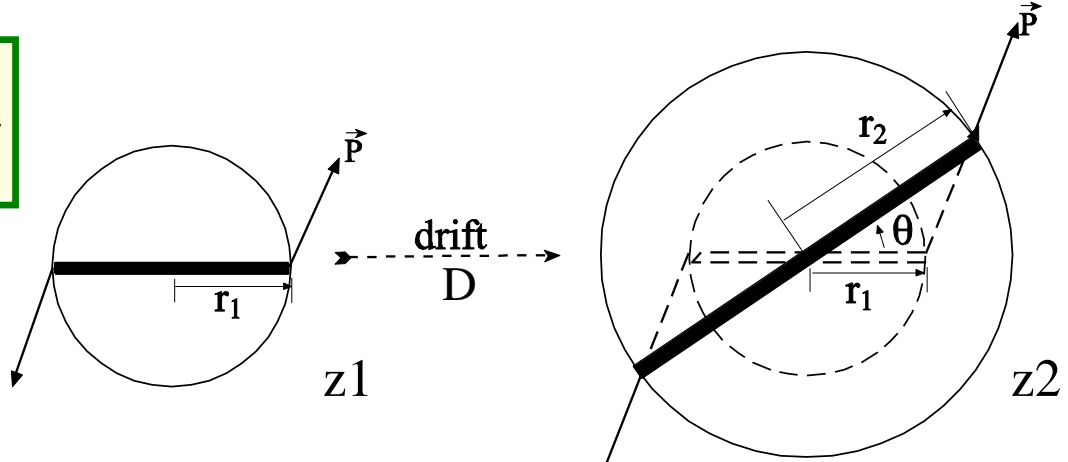
Solenoidal end field applies a torque to the beam.

When $B_z=0$, canonical = mechanical angular momentum.

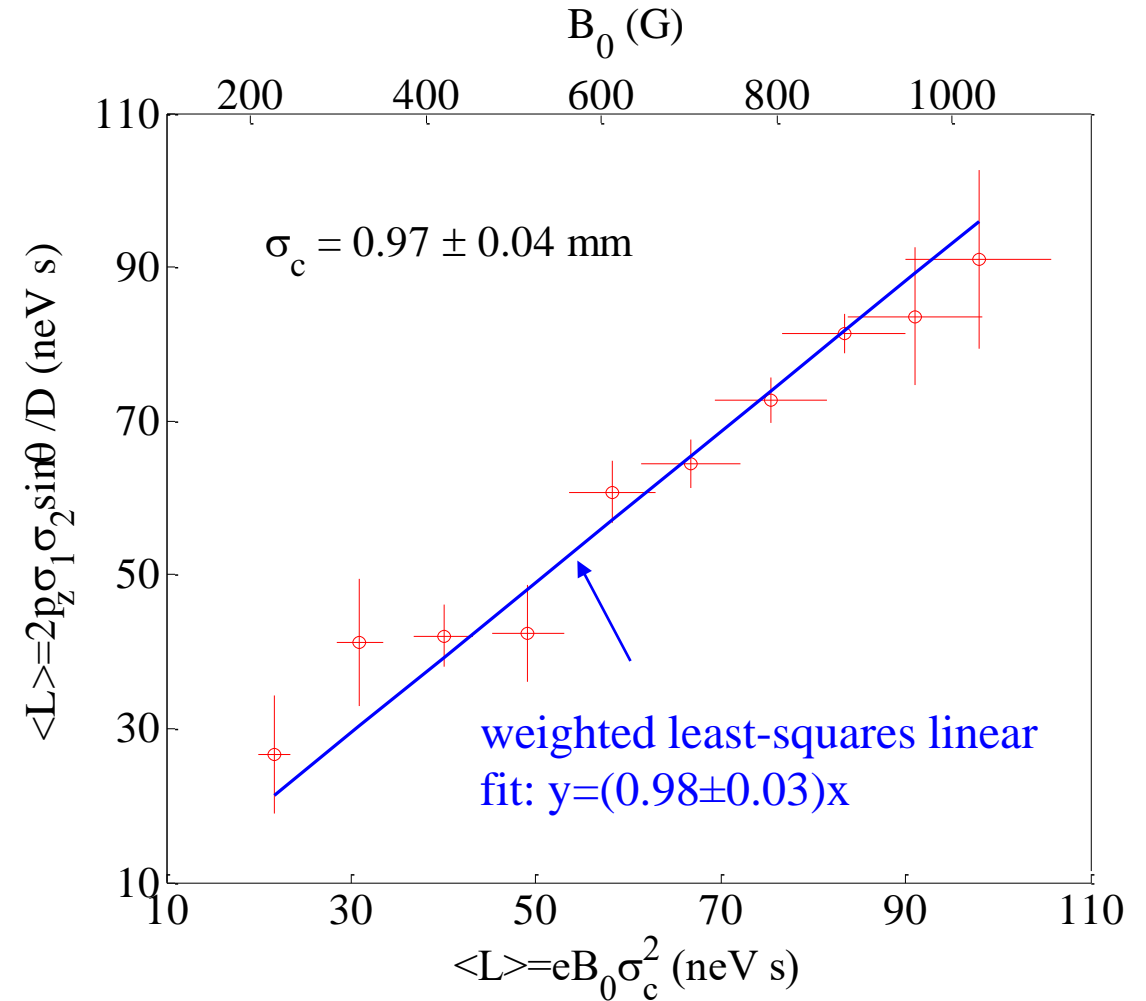
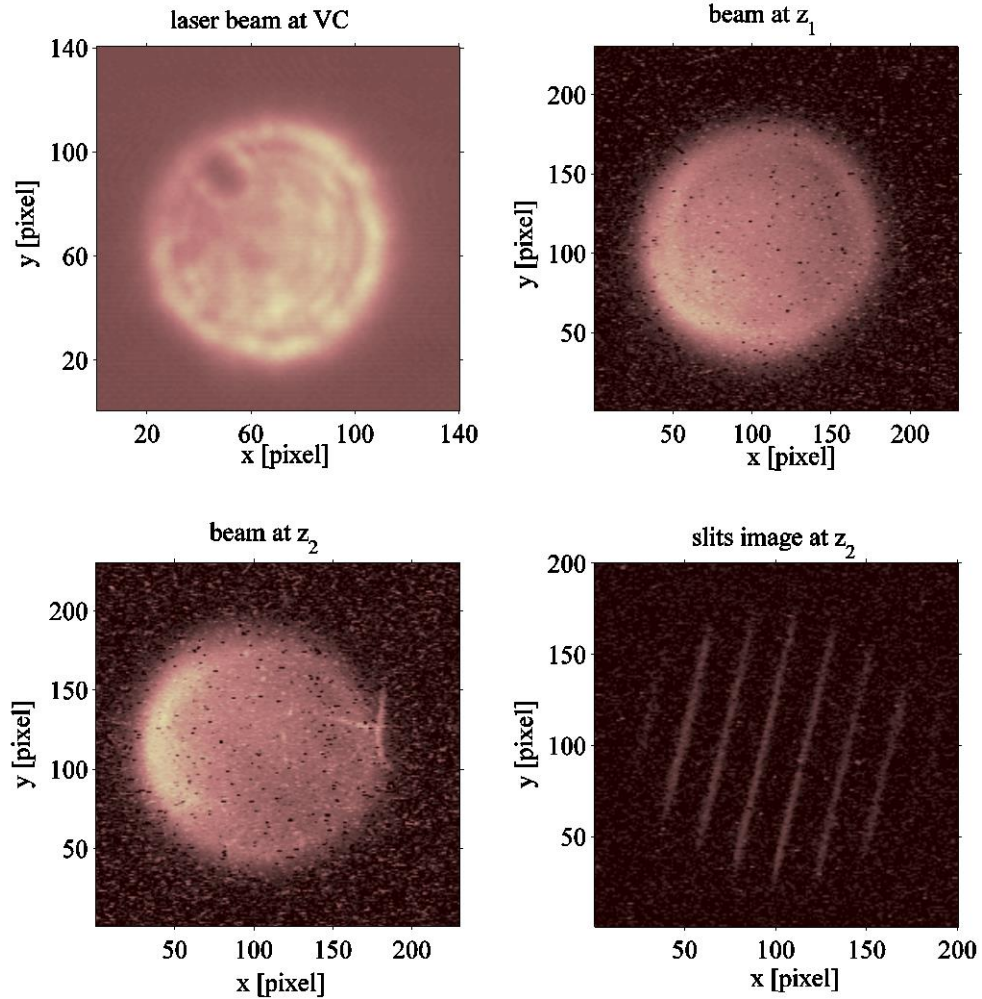
Measurement of canonical angular momentum in a drift space

- Insert flag or slits at Z1 →
- Measure beam size σ_1 at Z1
- Insert flag at Z2 →
- Measure beam size σ_2 and slits rotation angle θ at Z2

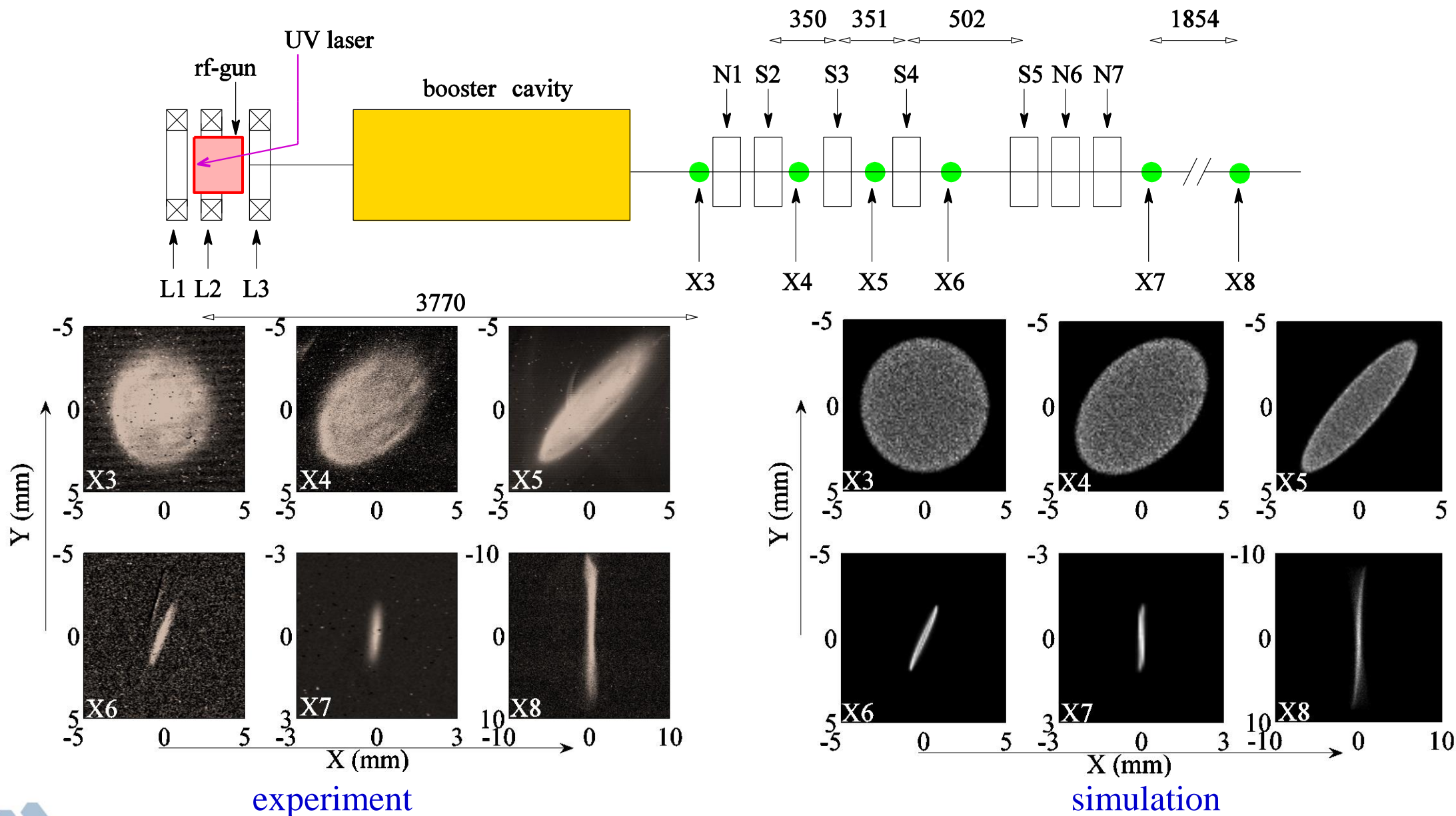
$$\langle L \rangle = 2 p_z \frac{\sigma_1 \sigma_2 \sin \theta}{D}$$



Demonstration of conservation of canonical angular momentum as a function of magnetic field on cathode



Removal of angular momentum and generating a flat beam



experiment

simulation

Compare Measurements with Simulation

	Experiment		Simulation
	90%	95%	(ASTRA)
rms_cathode(mm)		0.97	0.97
B_cathode(Gauss)		898	898
I_Quad1 (A)		-1.97	-1.98
I_Quad2 (A)		2.56	2.58
I_Quad3 (A)		-4.55	-5.08
rms_X7y (mm)	0.58±0.01	0.63±0.01	0.77
rms_X7x (mm)	0.084±0.001	0.095±0.001	0.058
rms_X8_hslit (mm)	1.57±0.01	1.68±0.01	1.50
rms_X8_vslit (mm)	0.12±0.01	0.13±0.01	0.11
Lcath (mm mrad)		24.5±0.7	
Lmech (mm mrad)		26.6±0.5	
Emit-uncorrelated (mm mrad)		5.1±0.7	
ϵ_x (mm mrad)	<u>0.39±0.02</u>	<u>0.49±0.02</u>	<u>0.27</u>
ϵ_y (mm mrad)	35.2±0.5	41.0±0.5	53
ϵ_y/ϵ_x	90±5	83±4	196
$(\epsilon_x \cdot \epsilon_y)^{0.5}$	3.7	4.5	3.8 mm mrad



Emittance EXchange



Transverse-to-Longitudinal Phase-Space Exchange

□ EEX theory:

- 2002: Cornacchia and Emma, PRSTAB 5, 084001.
 - Partial exchange : chicane
- 2006: Kim, AIP Conf. Proc. No. 821.
 - Complete exchange: double-dogleg

□ 2010: Double-dogleg EEX experiment demonstration:

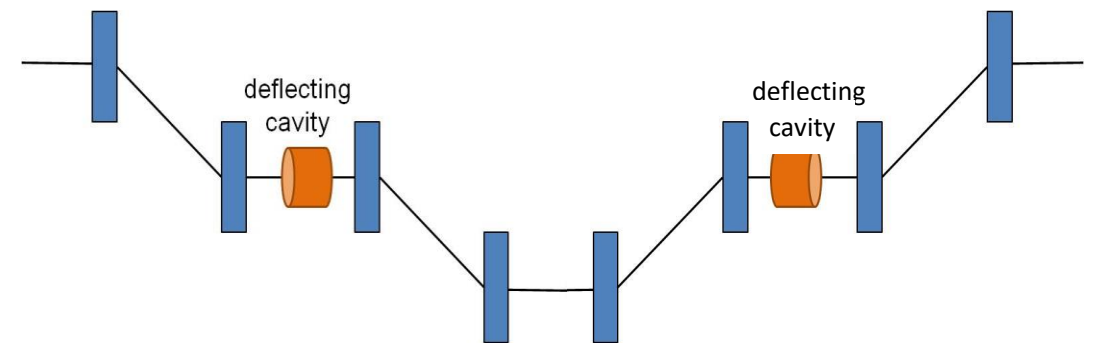
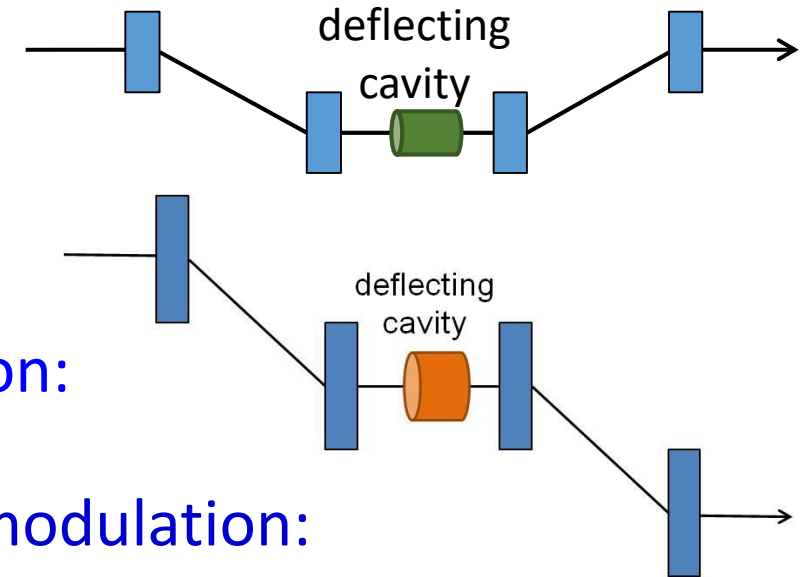
- J. Ruan et al., PRL 106, 244801 (2011).

□ 2010: Applications of EEX in beam current profile modulation:

- Y. Sun et al., PRL 105, 234801 (2010).
- G. Ha et al., IPAC2016, TUOBB01, TUPMY031(2016).

□ Double Emittance Exchange (DEEX)

- A. Zholents et al., ANL/APS/LS-327 (2011).

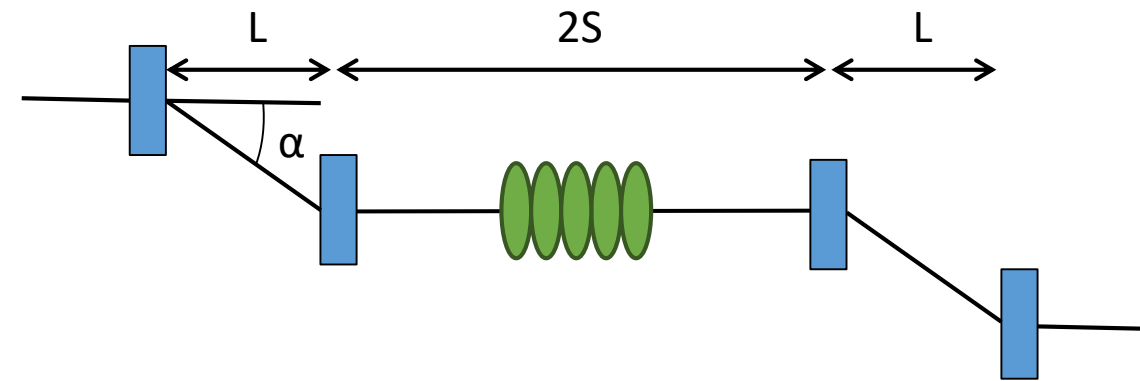


Transverse-to-Longitudinal Emittance EXchange

Four dipoles + one deflecting cavity:

Under thin-lens approximation, with proper matching of the deflecting cavity strength (k) and the dogleg dispersion (D), i.e., $1+kD=0$, the diagonal sub-block elements of the exchanger's transfer matrix are zero \leftrightarrow the initial horizontal phase space is mapped into the longitudinal phase space, vice versa.

With finite cavity length included, there will be non-zero terms in the diagonal blocks – which can be corrected by adding accelerating cells on the deflecting cavity [1], or reduced by adjusting initial beam transverse and longitudinal phase space correlations.

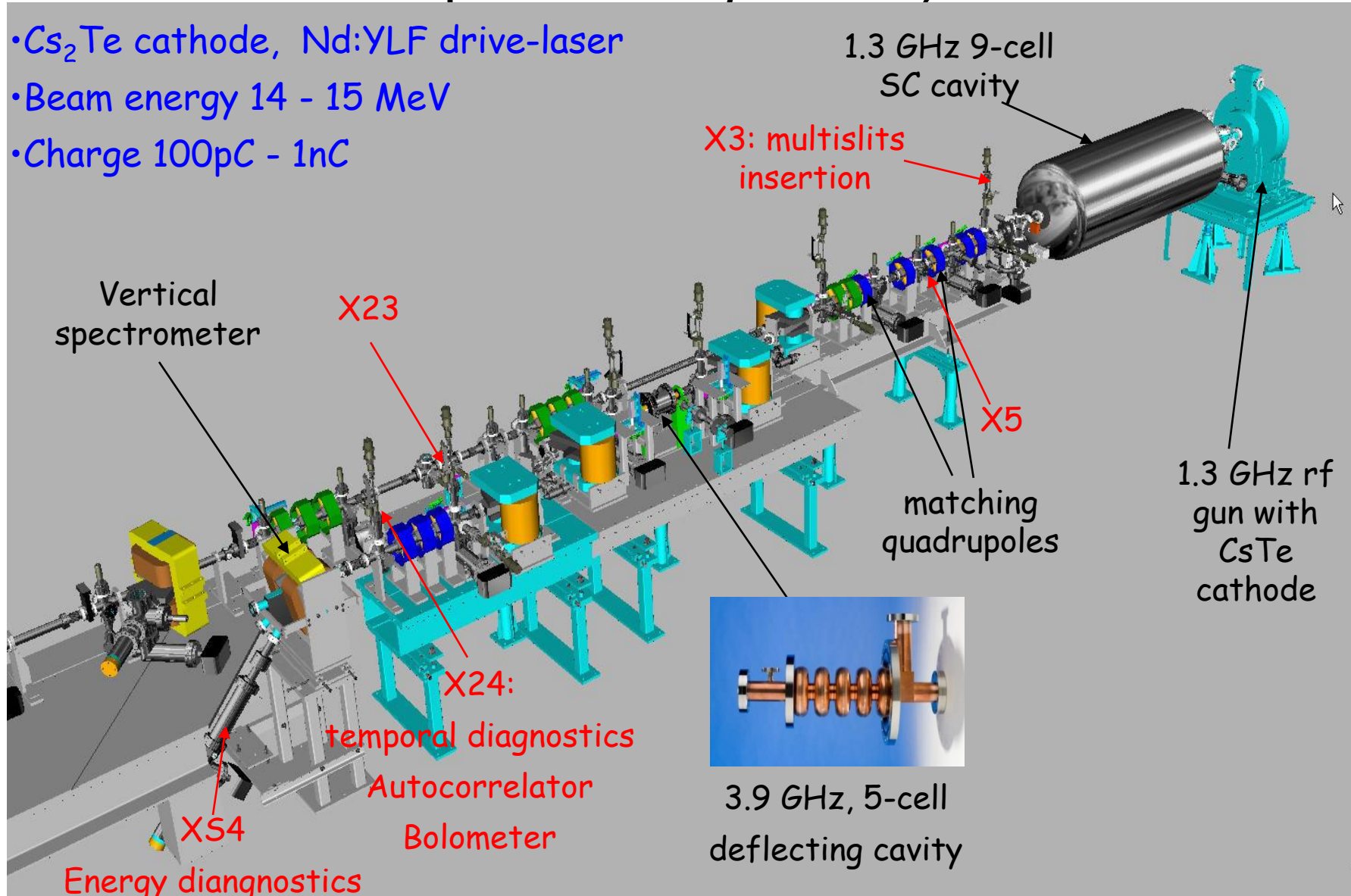


$$\begin{pmatrix} x \\ x' \\ z \\ \delta \end{pmatrix}_{out} = \begin{pmatrix} 0 & 0 & \frac{L+S}{\alpha L} & \alpha S \\ 0 & 0 & \frac{1}{\alpha L} & \alpha \\ \alpha & \alpha S & 0 & 0 \\ \frac{1}{\alpha L} & \frac{L+S}{\alpha L} & 0 & 0 \end{pmatrix} \begin{pmatrix} x \\ x' \\ z \\ \delta \end{pmatrix}_{in}$$

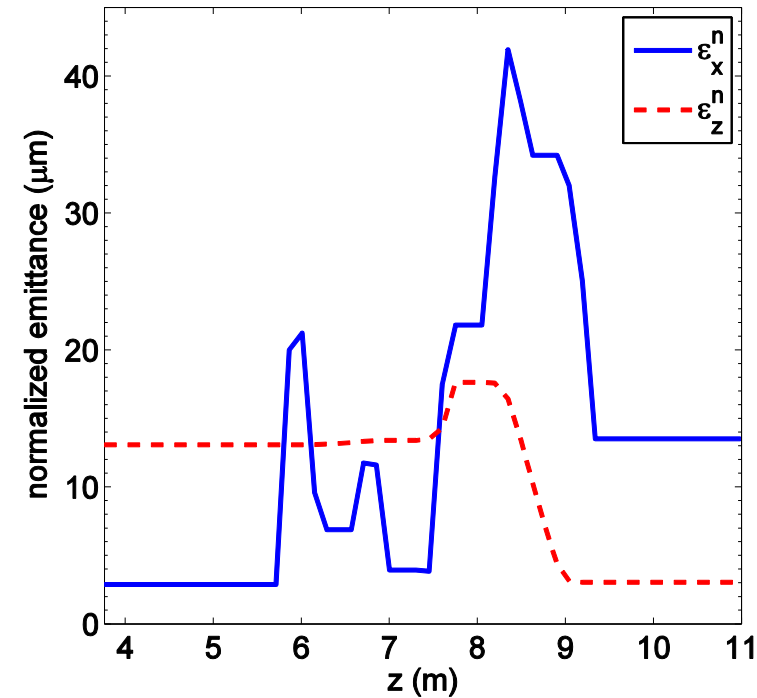
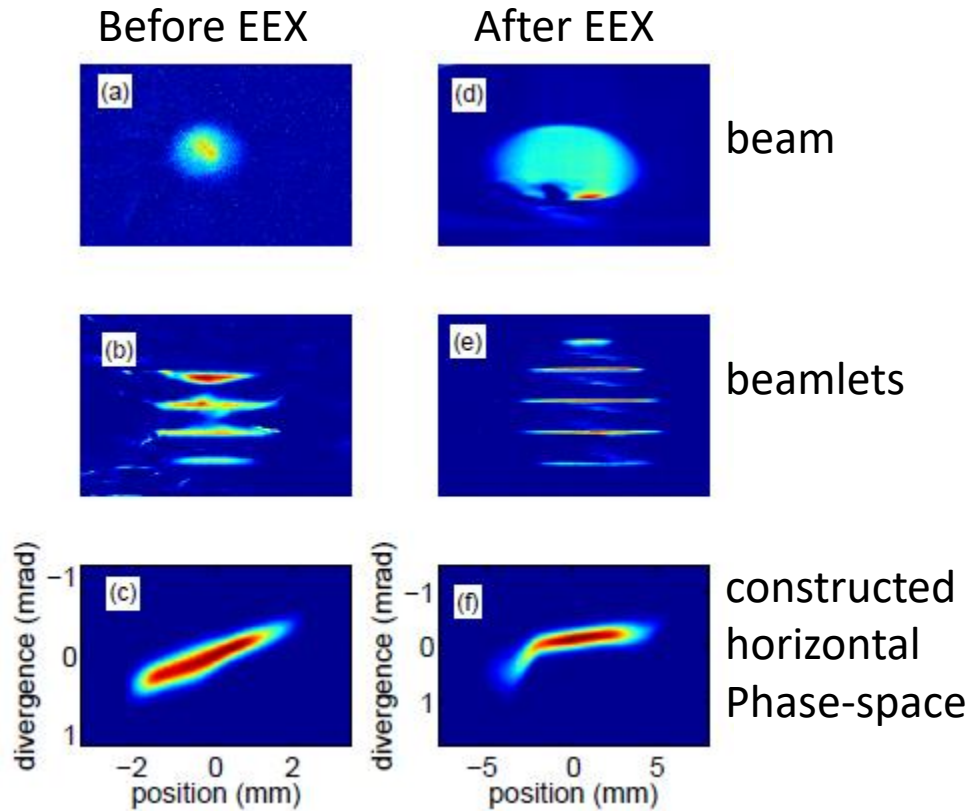
[1] A. Zholents, ANL/APS/LS-327, May 2011

EEX beamline at A0 photoinjector, Fermilab

- Cs₂Te cathode, Nd:YLF drive-laser
- Beam energy 14 - 15 MeV
- Charge 100pC - 1nC



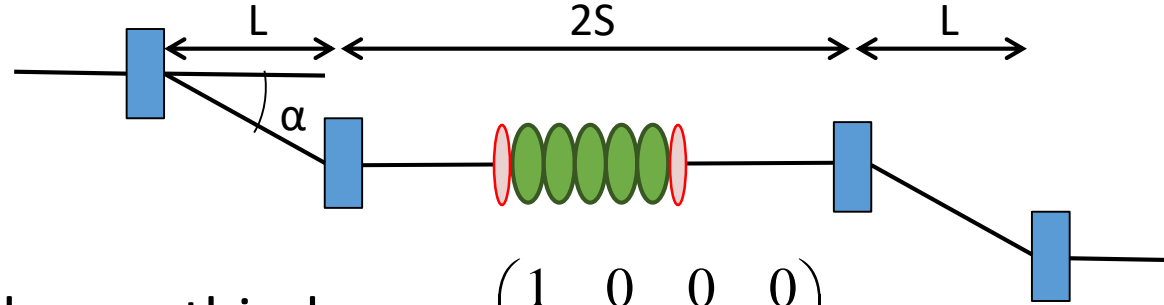
A0 EEX experiment and simulation at low charge



Norm. Emit.	Before EEX (exp.)	After EEX (exp.)	After EEX (simu.)
ϵ_x^n (μm)	2.9 ± 0.1	11.3 ± 1.1	13.5
ϵ_z^n (μm)	13.1 ± 1.3	3.1 ± 0.3	2.9
ϵ_y^n (μm)	2.4 ± 0.1	2.9 ± 0.5	3.0

J. Ruan, A. Johnson, Y.-E Sun, A Lumpkin, R. Thurman-Keup, FEL'2011, Shanghai, China

Thick-lens Effect



So far, only thin-lens approximation is considered for the transfer matrix of the deflecting cavity.

$$\begin{pmatrix} 1 & 0 & 0 & 0 \\ 0 & 1 & k & 0 \\ 0 & 0 & 1 & 0 \\ k & 0 & 0 & 1 \end{pmatrix}$$

When taking into account of the finite cavity length l , the matrix is

$$\begin{pmatrix} 1 & l & kl/2 & 0 \\ 0 & 1 & k & 0 \\ 0 & 0 & 1 & 0 \\ k & kl/2 & k^2l/6 & 1 \end{pmatrix}$$

The R_{43} leads to non-vanishing terms in the diagonal blocks of the EEX matrix.
Adding accelerating cavity to the deflecting cavity solves the problem.

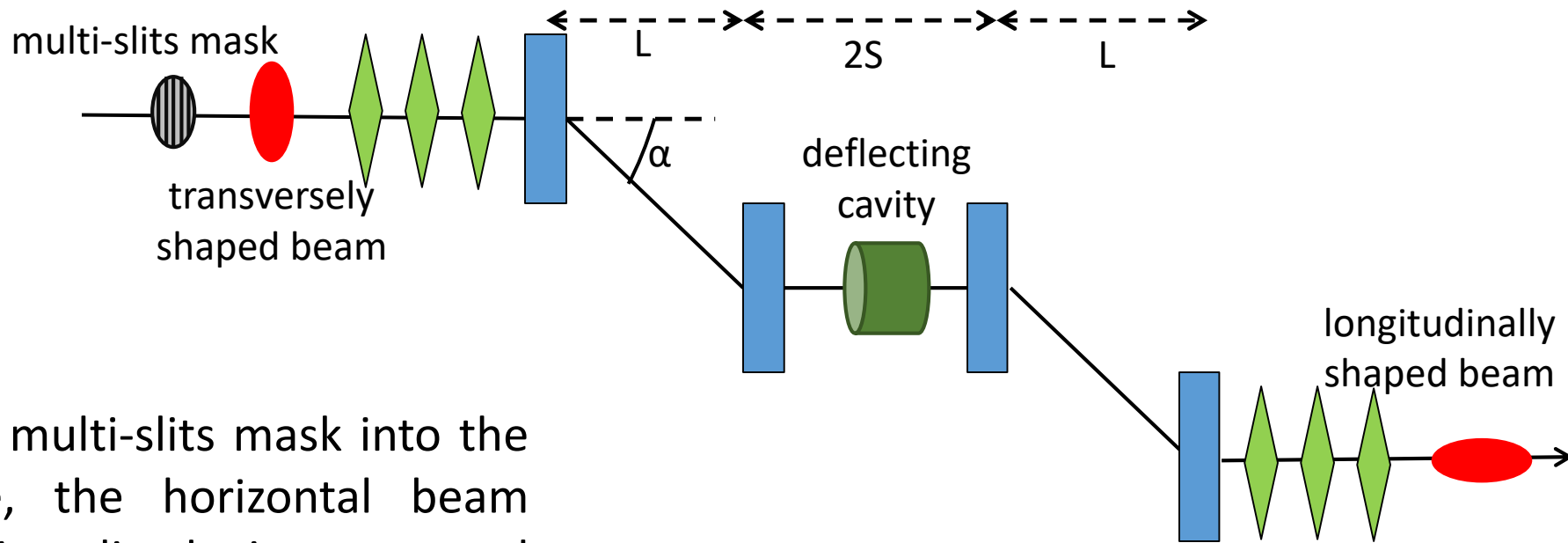
(A. Zholents, ANL/APS/LS-327, May 2011)

Longitudinal Phase Space Manipulation via EEX

-- bunch train generation



Longitudinal Shaping using EEX: sub-ps Bunch Train Generation



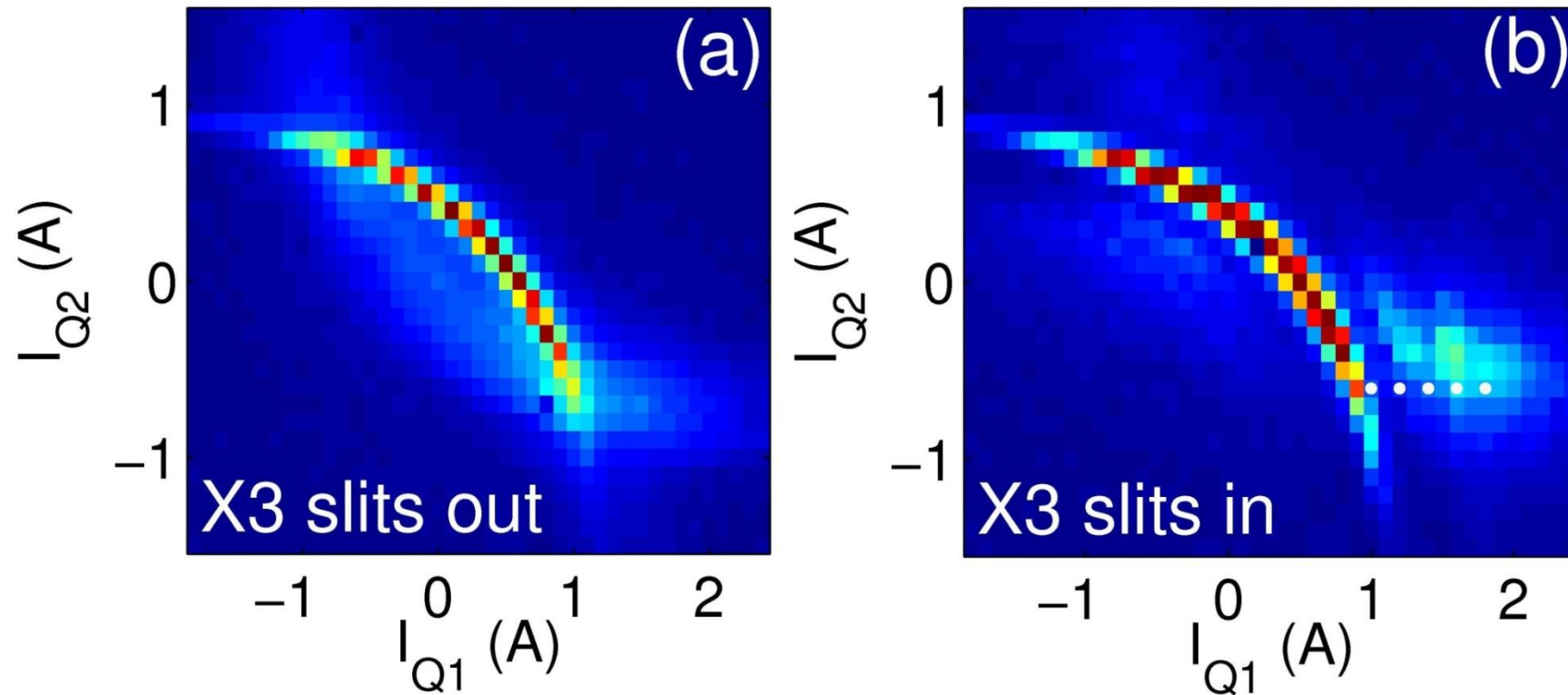
Inserting multi-slits mask into the beamline, the horizontal beam profile is sliced into several beamlets.

After the Phase-space Exchange (PEX), horizontal and longitudinal phase-space are swapped. Therefore, beam is now a bunch-train.

$$\begin{bmatrix} 0 & 0 & \frac{L+S}{L\alpha} & S\alpha \\ 0 & 0 & \frac{1}{L\alpha} & \alpha \\ \alpha & S\alpha & 0 & 0 \\ \frac{1}{L\alpha} & \frac{S\alpha}{L\alpha} & 0 & 0 \end{bmatrix} \Rightarrow \begin{bmatrix} z_f \\ \delta_f \end{bmatrix} = \begin{bmatrix} \alpha & S\alpha \\ \frac{1}{L\alpha} & \frac{S\alpha}{L\alpha} \end{bmatrix} \begin{bmatrix} x_i \\ x_i' \end{bmatrix}$$

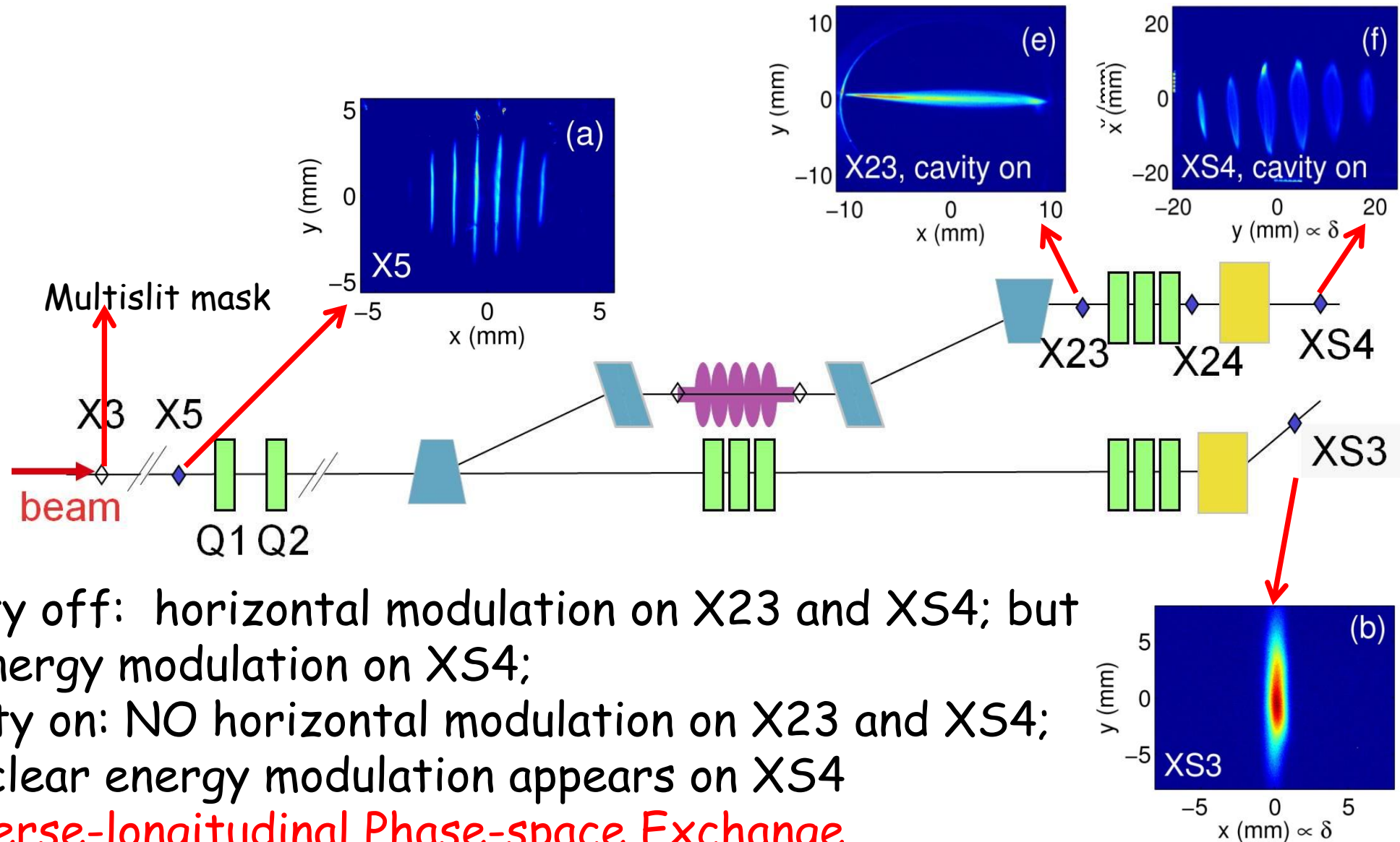
Quadrupoles before and after EEX to minimize the contribution from x_i' .

Final bunch length control via initial horizontal beam focusing



The final beam longitudinal properties can be controlled by initial horizontal beam parameters. While scanning the currents of two quadrupoles upstream of the double-dogleg beamline, the final bunch length after EEX can be monitored using an auto-correlator + bolometer system. Fig. (a) shows such a quadrupole scan without slits inserted, and (b) with the slits. The small island appeared with the slits inserted is related to the coherent radiation from the bunch-train.

Experimental demonstration of the sub-ps bunch train: energy domain

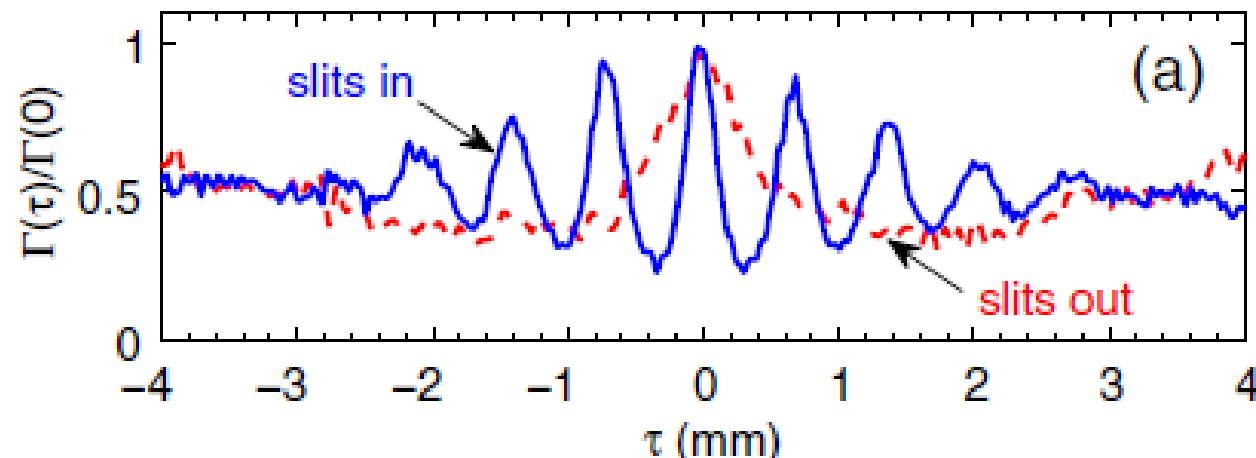


Experimental demonstration of the sub-ps bunch train: time domain

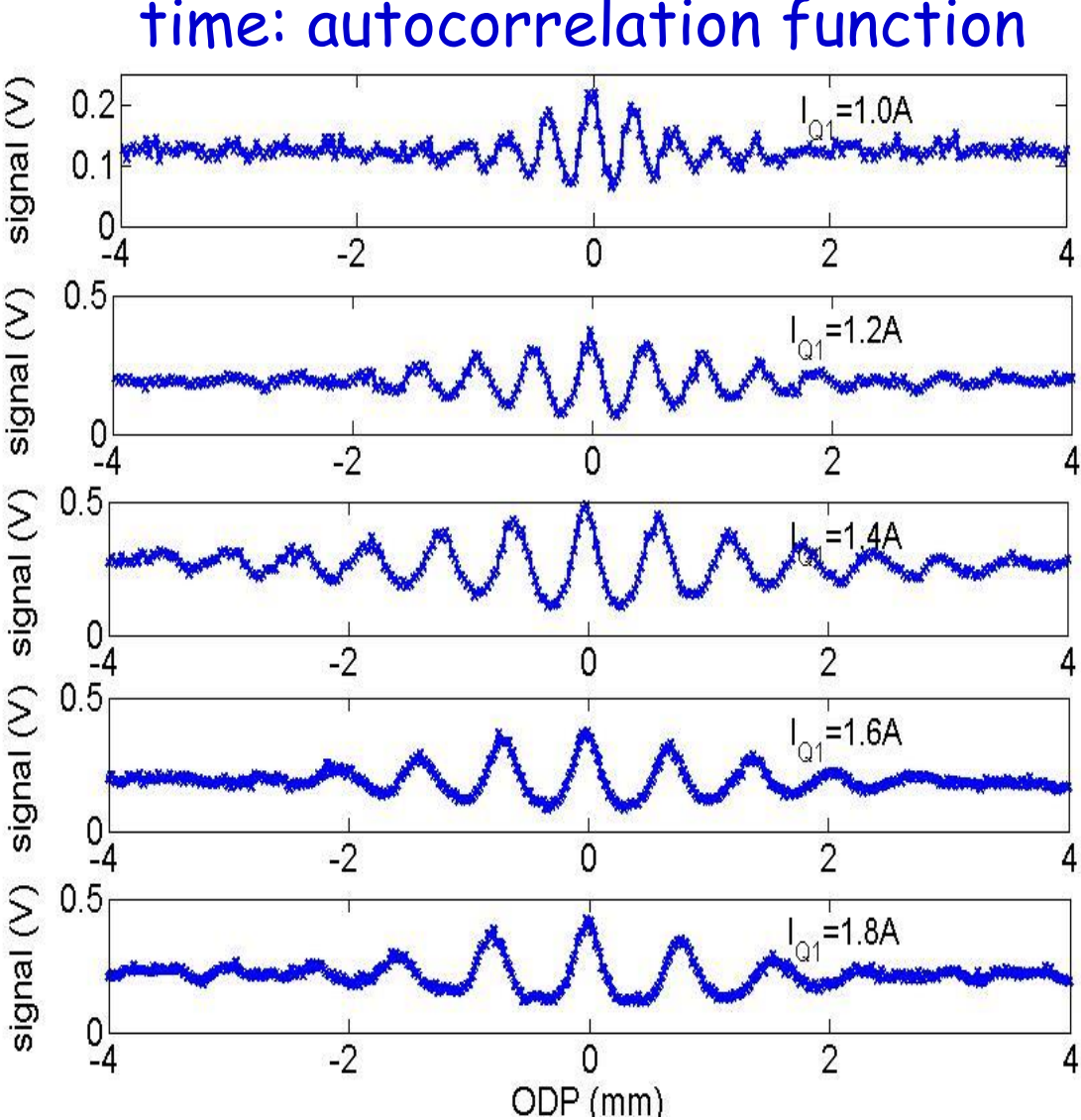
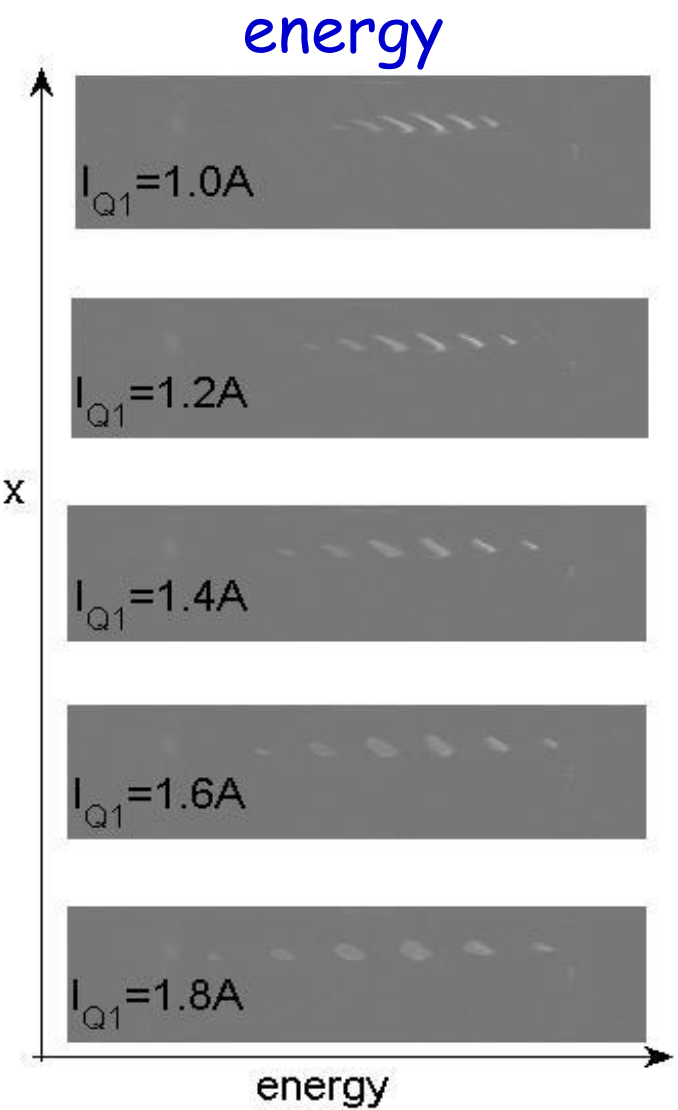
The bunch train temporal structure is measured via the CTR signal measured downstream of EEX.

A liquid-helium-cooled bolometer is used as the detector of the Michelson autocorrelator.

Multipeaks of the autocorrelation function are measured when the slit mask is inserted, compared to a single peak when the mask is out.



Experimental demonstration of the sub-ps bunch train



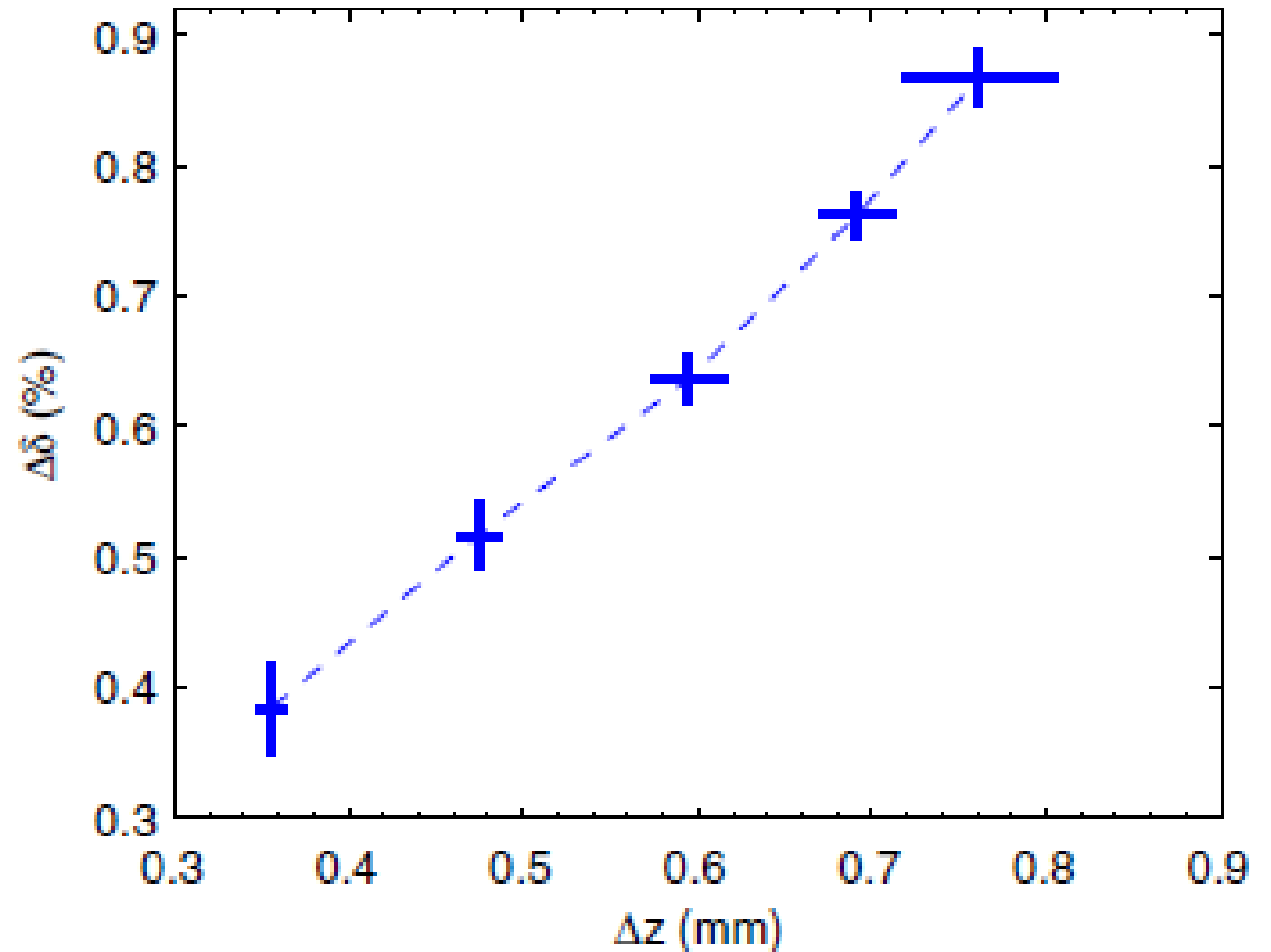
Y.-E Sun et al, PRL 105, 234801 (2010).

Experimental demonstration of the sub-ps bunch train: variable bunch separation

The bunch separation is extracted from the autocorrelation function to be [350 ~ 760] μm . The separation can be easily tuned by changing the currents of one single quadrupole upstream of EEX.

The corresponding CTR measured from these bunch trains is a narrow-band ($\delta f/f \approx 20\%$ at 0.5 THz) with tunable frequency of [0.37 0.86] THz. *

Assuming Gaussian distribution, the minimum individual bunch rms duration measured is less than 300 fs.



*P. Piot et al., *Applied Physics Letters* **98**, 261501 (2011)

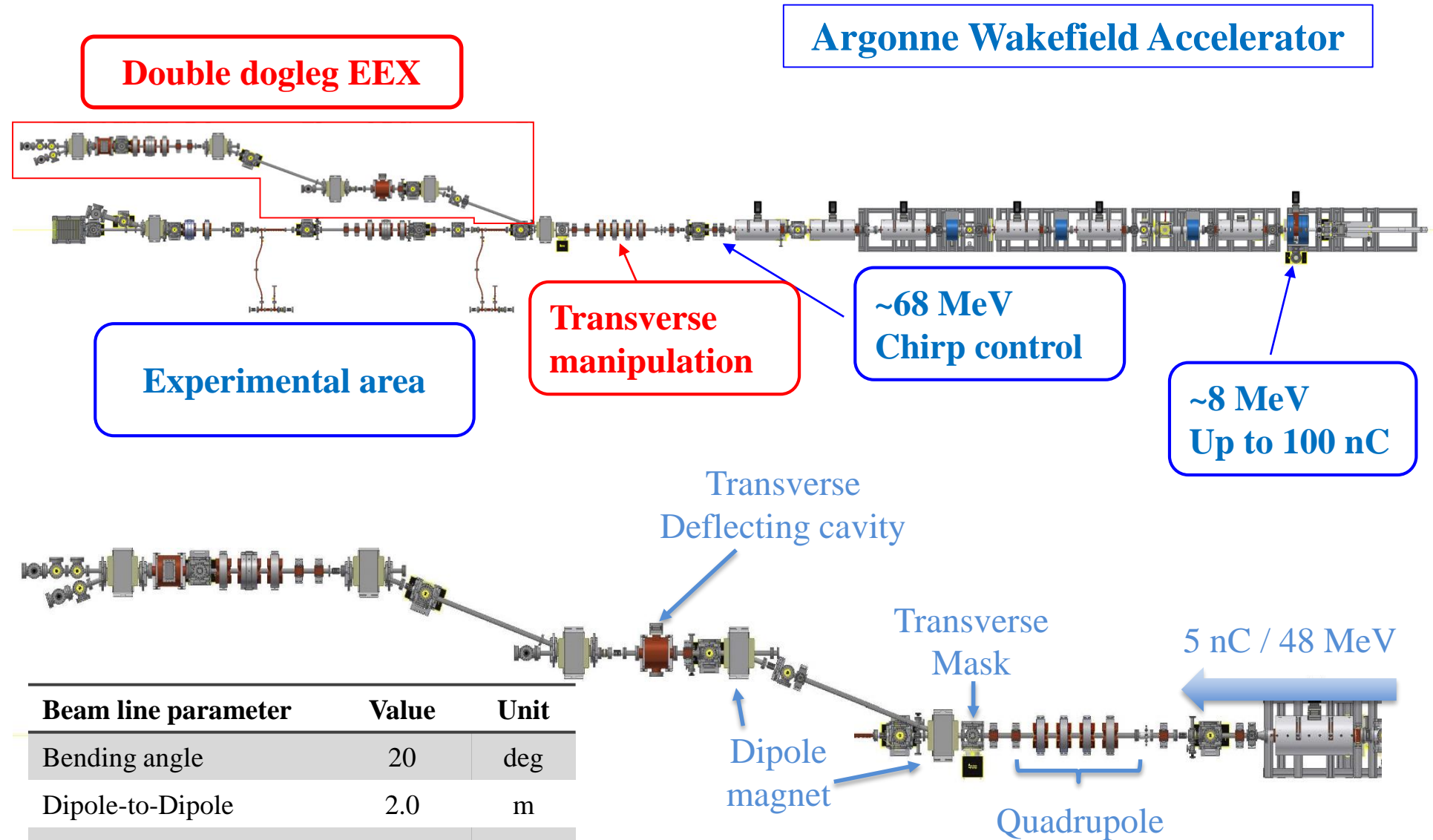
Longitudinal Bunch Shaping via EEX

-- Precise Beam Profile Control

Arbitrary Beam Longitudinal Beam Profile

- ❑ Transverse beam shaping is mature. Tools to obtain desired transverse beam profile include shaping the drive-laser transverse profile for a photo-injector, inserting masks in the beam path, using quadrupoles to focus/defocus etc.
- ❑ Longitudinal shaping techniques to achieve arbitrary beam profile are rather limited relative to transverse shaping.
- ❑ EEX offers an opportunity to shape the beam transversely and then convert it to longitudinal – recently demonstrated at the Argonne Wakefield Accelerator (AWA/ANL).

Double dogleg EEX beam line at AWA (Slide from J. Power, AAC2016)

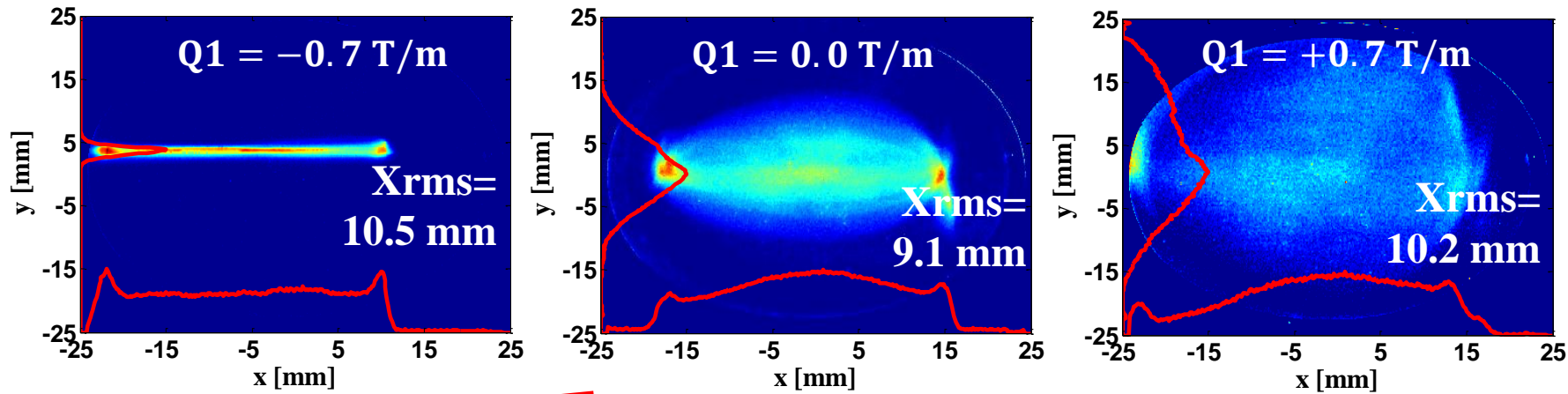


Beam line parameter	Value	Unit
Bending angle	20	deg
Dipole-to-Dipole	2.0	m
Dipole-to-TDC	0.5	m
Power to TDC	1.2	MW

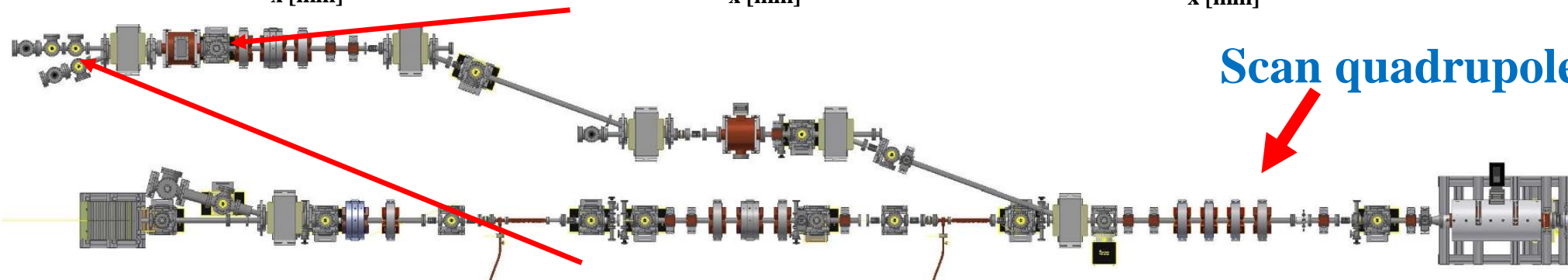


Demonstration of property exchange (Slide from J. Power, AAC2016)

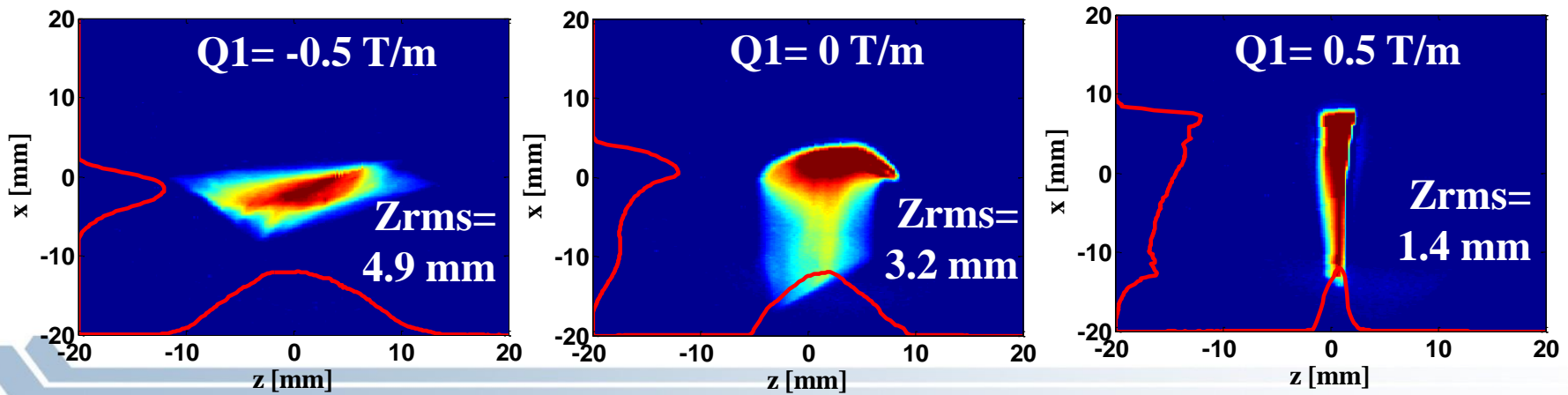
EXPERIMENT: Quad strength controls bunch length instead of horizontal beam size



X_{rms} : small variation



Scan quadrupole strength



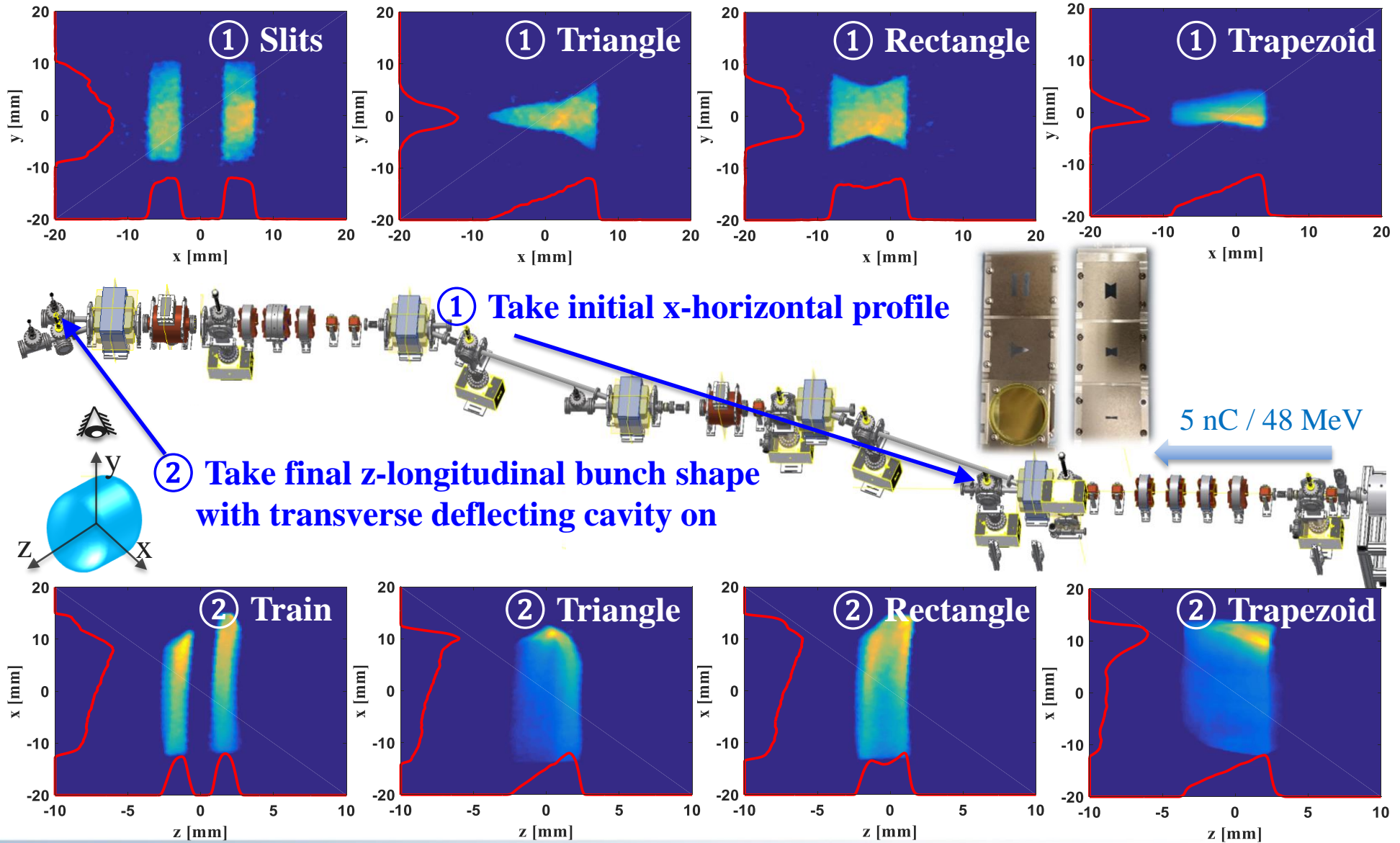
Z_{rms} : large variation



Demonstration of longitudinal bunch shaping at AWA/ANL

G. Ha et al,
to appear in *Physics Review Letters*

EXPERIMENT: Transverse mask to tailor longitudinal density profile



6D Phase-Space Manipulation

□ Single-stage EEX:

- The double-dogleg EEX approach leave the beam line with a transverse offset, not desired in a straight linac accelerator tunnel;
- As the transverse and longitudinal phase space exchange only once, the final transverse emittance might be larger than before the EEX – which may not be a desired feature for some applications.

□ Double-stage EEX*

- Adding another double-dogleg EEX as a second stage will solve the two issues encountered above.
- In between the two stages of EEX, mature transverse phase space manipulation techniques can be deployed to create final longitudinal phase space.

□ Round-Flat beam transformation + EEX → Arbitrary 6D phase-space manipulation

- Round-to-flat beam transformation between the two transverse phase spaces;
- Transverse-to-longitudinal EEX between any transverses phase space and the longitudinal phase space.

[*]A. Zholents et al., ANL/APS/LS-327 (2011)

